

See discussions, stats, and author profiles for this publication at: <https://www.researchgate.net/publication/287929162>

Artificial Viscosity Methods for Modelling Shock Wave Propagation

Article · June 2009

DOI: 10.1007/978-1-4419-0727-1_19

CITATIONS

3

READS

113

2 authors:



James Campbell
Brunel University London

61 PUBLICATIONS 932 CITATIONS

[SEE PROFILE](#)



Rade Vignjevic
Brunel University London

104 PUBLICATIONS 1,242 CITATIONS

[SEE PROFILE](#)

Some of the authors of this publication are also working on these related projects:



RACEForm - (Rapid aluminium cost-effective forming), Innovate UK / APC7 Grant [View project](#)



NetDeliver: Network on numerical modeling and simulation of anticancer drug delivery in liver [View project](#)

Artificial Viscosity Methods for Modelling Shock Wave Propagation

James Campbell and Rade Vignjevic

Abstract The paper gives an overview of the artificial viscosity method widely used today to allow the simulation of problems containing shock waves. The development of the most common basic form of the viscosity term is summarised and its behaviour is illustrated through simulations of a 1D piston problem. Test problems that are commonly used to test different viscosity formulations are then discussed to further illustrate the method. Finally other shock viscosity forms such as edge and tensor viscosities are briefly discussed.

1 Introduction

The requirement to model shock wave propagation has been around since the earliest days of hydrocodes, with finite difference simulations used at Los Alamos during the Manhattan project in order to study the behaviour of shock waves. An understanding of shock propagation was critical for the design of the atomic bomb.

A shock wave has a thickness of the order of a few molecular mean free paths. This is a very small dimension, much smaller than the typical length scale considered in continuum mechanics simulations. It is completely impractical to consider modelling a macroscopic problem with a mesh size small enough to resolve this. The result is that a shock represents a discontinuity in the solution, a surface over which there is a jump in velocity, pressure, density and energy.

One possible approach is to treat the shock as an interface between two regions of the flow. In this approach the Hugoniot equations along with the material's Equation

James Campbell
Cranfield University, School of Engineering - Applied Mechanics, Cranfield, Bedford, UK, e-mail:
j.campbell@cranfield.ac.uk

Rade Vignjevic
Cranfield University, School of Engineering - Applied Mechanics, Cranfield, Bedford, UK, e-mail:
v.rade@cranfield.ac.uk

of State (EOS) can be used to solve for the jump in solution variables across the shock. These values are then applied as boundary conditions to the two regions of flow. This approach can be used in one dimensional simulations, but in two- or three-dimensional simulations it is impractical as the shock represents a moving interface of potentially complex shape. Tracking this potentially arbitrary boundary accurately, and applying the necessary jump conditions over the interface represents a complex numerical and algorithmic challenge.

Two well established methods exist today for the treatment of shocks within numerical simulations:

- Artificial viscosity
- Godunov's method

The artificial viscosity concept, developed by von Neumann and Richtmyer [1], allowed the first practical numerical simulations of problems containing strong shocks. The concept involves the introduction into the numerical scheme of a viscosity-like term that acts to spread the thickness of any shock wave over several mesh cells. As the shock no longer represents a discontinuity in the solution, standard numerical methods can be used to simulate the shock propagation. This approach has proved to be simple and robust, accounting for its continuing use today. The drawbacks of the method is that it can introduce an unacceptable degree of mesh sensitivity into the solution and there is a trade-off between shock thickness and degree of oscillation behind the shock.

Godunov's method [2] and the class of numerical methods developed from it represent an entirely different approach. In summary Godunov's method assumes that all solution variables within a cell are constant at the start of a step, with discontinuities occurring at the edges of a cell treated through the solution of a Riemann problem. This approach allows the shocks in the solution to be physically and naturally treated. The drawback is the high numerical cost of solving the Riemann problem. This has required the use of approximate Riemann solvers which introduce further approximations into the numerical method. Even approximate solutions of the Riemann problem remain expensive when complex equations of state are required, which has effectively limited the common application of the methods to fluid mechanics simulations. In addition, like the artificial viscosity method, it introduces mesh sensitivity into the solution. Further information on Godunov's method and Riemann solvers can be found in Toro [3].

2 The Von Neumann - Richtmyer viscosity

The governing equations of Lagrangian hydrodynamics are the momentum (1), the energy (2) and the continuity (3) equations:

$$\rho \frac{d\mathbf{v}}{dt} = \nabla \cdot \boldsymbol{\sigma} , \quad (1)$$

$$\rho \frac{de}{dt} = \sigma : \mathbf{D}, \quad (2)$$

$$\frac{d\rho}{dt} = -\rho \nabla \cdot \mathbf{v} \quad (3)$$

where ρ is density, σ is the stress tensor, \mathbf{v} is the velocity vector, e is the specific internal energy. \mathbf{D} is the rate-of-deformation tensor defined as the skew symmetric part of \mathbf{L} , the velocity gradient tensor:

$$\mathbf{L} = (\nabla \mathbf{v})^T \quad \text{and} \quad \mathbf{D} = \frac{1}{2}(\mathbf{L} + \mathbf{L}^T) \quad (4)$$

The approach taken by Von Neumann and Richtmyer [1] for one dimensional shock wave calculations was to modify the momentum and energy equations by adding a dissipative, viscosity like, term q to the stress tensor. Introducing this term into the governing equation acts to smear out the shock so as to produce a thickness of the order of the resolution length of the computational mesh. A particular feature of this approach is that the term is added to the equations throughout the computational domain, not just where a shock is present, removing the need to track shocks. As the dissipative term is added for purely mathematical reasons, it can be any function that satisfies the following constraints [1]:

1. The modified conservation equations (1-3) must possess solutions without discontinuities.
2. The thickness of a shock must everywhere be of the order of the resolution length of the mesh, independent of the strength of the shock.
3. The dissipative term must be negligible outside of the shock wave.
4. The Hugoniot equations must hold when all other dimensions are large compared to the shock thickness.

The expression proposed by Von Neumann and Richmyer for their viscosity is written for the one-dimensional case as

$$q = -\rho(c\Delta x)^2 \frac{\partial v}{\partial x} \left| \frac{\partial v}{\partial x} \right|, \quad (5)$$

where c is a dimensionless constant. The viscous term q is then included in the solution by replacing the stress, σ , in the governing equations by $(\sigma - q\mathbf{I})$. This term is quadratic in the velocity gradient and is positive in compression and negative in tension. As the viscosity term is not required in expansion it is common to set $q = 0$ when $\frac{\partial v}{\partial x} > 0$.

The Von Neumann-Richtmyer q shown in equation (5) does work effectively, and with a value of c of the order of 2 will spread a shock over three to five mesh cells [4]. Its disadvantage is that any oscillation that does occur behind the shock is only slowly damped out and lowering the value of c to reduce the thickness of the shock results in an overshoot that produces oscillation. To address this problem Landshoff [5] proposed an expression for q that was linear in the velocity gradient. This term vanishes less rapidly behind a shock front and so rapidly damps out the

oscillation, but as the term is smaller in the shock front itself much larger overshoots occur. Landshoff recommended that the two terms be combined to produce a q that combines the best features of each:

$$q = -\rho c_L \Delta x a \left| \frac{\partial v}{\partial x} \right| - \rho c_Q (\Delta x)^2 \frac{\partial v}{\partial x} \left| \frac{\partial v}{\partial x} \right|, \quad (6)$$

where a is the local speed of sound and c_L and c_Q are dimensionless constants that multiply the linear and quadratic terms respectively. This basic form of viscosity proved effective and is still widely used today.

Extending the one-dimensional form of the viscosity (6) to two or three dimensions requires appropriate definitions of the velocity gradient and the characteristic length. It is common to follow the original idea of Von Neumann and Richtmyer [1] by replacing the velocity gradient term with the trace of the rate-of-deformation tensor:

$$\begin{aligned} q &= -\rho c_L l a \dot{D}_{kk} - \rho c_Q l^2 \dot{D}_{kk}^2 && \text{if } \dot{D}_{kk} < 0 \\ q &= 0 && \text{if } \dot{D}_{kk} \geq 0 \end{aligned} \quad (7)$$

The definition of the characteristic grid length, l , is not so simple. Ideally the characteristic length used would be the element thickness in the shock propagation direction, but calculating this for all elements every step is difficult and costly. The usual approximation used in three dimensions is the cube root of the volume, $\sqrt[3]{V}$, and in two dimensions the square root of the area, \sqrt{A} . These values are simple and quick to calculate and provide a good estimate of the critical length provided the aspect ratios of the elements are close to one. As the element aspect ratio becomes poor the use of these estimates leads to increasing unphysical behaviour and even numerical problems.

2.1 Demonstration

The behaviour of the von Neuman-Richtmyer viscosity will now be illustrated through simulations of a 1D piston problem. In this problem a box with an initial length of 1 is filled with a cold perfect gas with $\gamma = 5/3$ and initial density $\rho_0 = 1.0$. The right hand end of the box is fixed, while the left hand end is a piston that moves into the box with a fixed velocity of 1.0. A shock of infinite strength ($P_0 = 0$) is generated by the piston motion and moves into the gas ahead of the piston, figure 1.

An exact solution to this problem can be obtained using the Hugoniot relations that connect the state ahead of the shock with the state behind:

$$v_s = \frac{(v_1 - v_0)\rho_1}{\rho_1 - \rho_0}, \quad (8)$$

$$P_1 - P_0 = \rho_0 v_s (v_1 - v_0), \quad (9)$$

Fig. 1 Diagram of the 1D piston problem, showing the state of the gas ahead and behind the shock.

$$e_1 - e_0 = \frac{P_1 + P_0}{2} \left(\frac{1}{\rho_0} - \frac{1}{\rho_1} \right). \quad (10)$$

These equations link the density, ρ , pressure, P , specific internal energy, e , and particle velocity, v , across a shock travelling with velocity v_s . The state ahead of the shock is denoted with subscript 0 and behind the shock with subscript 1.

To calculate the exact solution for this problem a fourth equation is required, the perfect gas equation of state:

$$P = (\gamma - 1)\rho e. \quad (11)$$

These equations can now be solved explicitly to derive an expression for the pressure jump across the shock in terms of the conditions ahead of the shock and the change in particle velocity across the shock:

$$P_1 = P_0 + \rho_0 \frac{(\gamma + 1)}{4} (\Delta \mathbf{v})^2 + \rho_0 |\Delta \mathbf{v}| \sqrt{\left(\frac{\gamma + 1}{4} \right)^2 (\Delta \mathbf{v})^2 + a_0^2}, \quad (12)$$

where a is the local speed of sound given by

$$a = \sqrt{\frac{\gamma P}{\rho}} \quad (13)$$

The conditions ahead and behind the shock and the shock speed are given in 1.

Figures 2 to 6 show results from several simulations of this problem with varying c_L and c_Q . All the simulations were performed using the DYNA Lagrangian hydrocode [6], using the standard form of viscosity given by equation (7). The model consists of 100 elements along the length of the box. Eight node hexahedral continuum elements were used, along with symmetry boundary conditions to enforce a state of uni-axial strain. All the elements are perfect cubes at the start of the problem so $l = \sqrt[3]{V}$ is a good measurement of the critical length. All the results are shown as plots of element pressure vs. element coordinate at time $t = 0.7$. At this point the piston coordinate 0.7 and the shock coordinate is 0.93.

The first simulation, figure 2, shows a result using the quadratic term only with a small coefficient ($c_L = 0.0$ and $c_Q = 0.5$). The overshoot and oscillation behind the shock can be clearly seen and is only slowly damped. In a practical analysis the level of noise in this solution would not be acceptable. Increasing the value of the quadratic coefficient reduces the level of overshoot and hence the oscillation

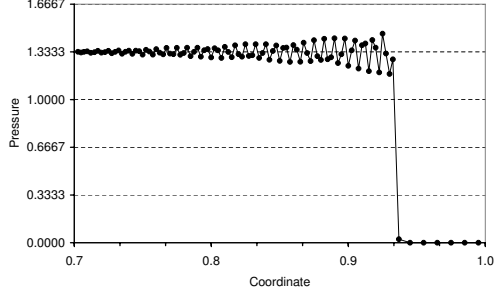


Fig. 2 Pressure profile for piston problem at time $t = 0.7$, with $c_L = 0.0$ and $c_Q = 0.5$.

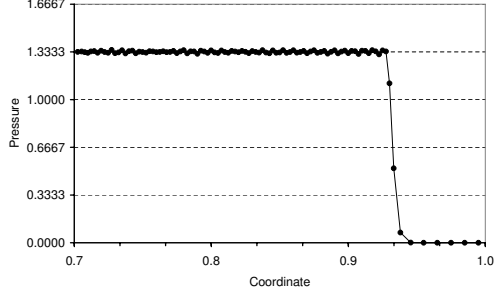


Fig. 3 Pressure profile for piston problem at time $t = 0.7$, with $c_L = 0.0$ and $c_Q = 2.0$.

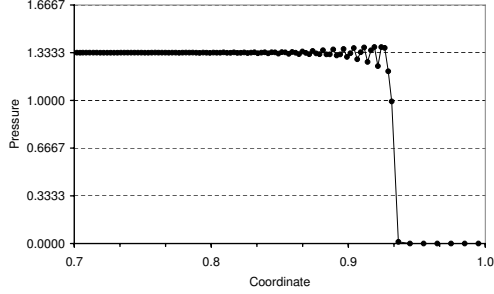


Fig. 4 Pressure profile for piston problem at time $t = 0.7$, with $c_L = 0.1$ and $c_Q = 0.5$.

as can be seen in figure 3 ($c_L = 0.0$ and $c_Q = 2.0$). Here the solution behind the shock is good, but at the cost of a wider shock front. The effect of introducing the linear term is to more rapidly damp out the oscillations behind the shock as can be seen in figure 4 ($c_L = 0.1$ and $c_Q = 0.5$). Here even a fairly small value for the linear coefficient results in a much more rapid damping behind the shock with only a small increase in the width. Increasing the linear coefficient eventually results in

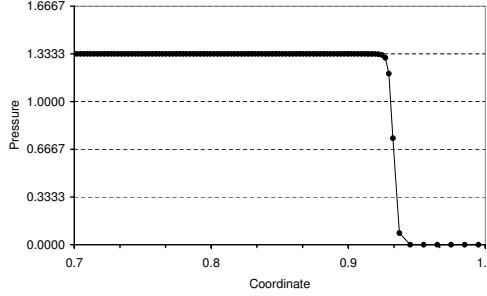


Fig. 5 Pressure profile for piston problem at time $t = 0.7$, with $c_L = 1.0$ and $c_Q = 0.5$.

a monotonic profile with no overshoot behind the shock but again at the cost of a wider front, figure 5.

Today, in a 1D calculation like this, the width of the shock front is not a problem as the computational cost of each simulation is negligible and a high spatial resolution can be used. In 3D models it is still desirable to keep the width of the shock as small as practical as increasing the spatial resolution can easily result in models that are too computationally expensive to use.

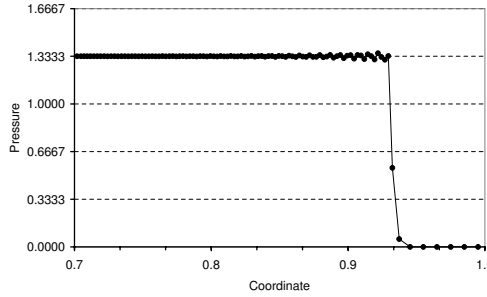


Fig. 6 Pressure profile for piston problem at time $t = 0.7$, with $c_L = 0.06$ and $c_Q = 1.5$.

There is a further and more serious problem with artificial viscosity that must be considered when selecting the values of the two coefficients. This problem was studied by Noh who called it shockless Q heating [7]. The viscosity term is non-zero everywhere where compression occurs and this leads to error in the solution where the assumption that the dissipative term is negligible outside the shock wave does not hold. Due to this error, as the linear term is larger than the quadratic term when \dot{D}_{kk} is small, it is common to keep the value of the linear coefficient small. The default values used in the DYNA code are $c_L = 0.06$ and $c_Q = 1.5$ [6], experience has shown that these values provide a reasonable balance between shock thickness and oscillation behind the shock for many cases. Results for the piston problem using these coefficients are shown in figure 6. The value of the quadratic coefficient

results in a reasonably sharp shock front with a small overshoot and small linear term damps out the oscillation behind the shock.

2.2 Wall Heating

This is an error that occurs on shock formation, for example at the start of the piston problem. It manifests in the solution as region where the density is underestimated and the internal energy overestimated. While this problem has been known and studied since the early days of shock computations, the now common name wall heating comes from the study by Noh [7]. He showed that this error is unavoidable as it is present in the solution of the governing differential equations containing a q term. The presence of this error is often ignored as often it only affects the solution in a small region and does not threaten the overall stability of the calculation. However in some particular applications, such as when the shock is generated at the centre of convergent geometry, the error can be significant and so solutions have been proposed, an example is the artificial heat flux term developed by Noh [7] to smear out this error. This error is still investigated; see for example Rider [8] for a more recent study.

3 Test problems for shock viscosity formulations

Since its original development many different forms for the artificial viscosity term have been proposed. The motivation has included improving the solution near the shock and in particular reducing the mesh sensitivity introduced when the original 1-D formulation has been extended to 2- and 3- dimensions. In principle any problem involving shock propagation can be used to investigate the properties of a shock viscosity, but one result of the continued development has been the emergence of certain test problems that are more commonly used to test or illustrate different formulations. Three problems will now be considered in more detail: the Sod shock tube [9], the Noh problem [7] and the Saltzman piston problem [11]. Other test problems that are used include the Sedov blast wave [10], uniform compression [7] and the Coggeshall adiabatic compression problem [10].

3.1 Sod shock tube

In addition to the piston problem used previously another commonly used 1D problem is the Sod shock tube problem, named after Gary Sod who used this problem to investigate the performance of several numerical methods [9]. This problem consists of two regions of perfect gas with different initial densities and pressures, figure 7.

In both regions the gas is initially at rest. The solution consists of a rarefaction wave that travels to the left, a contact discontinuity and a shock that travels to the right. In both regions the ratio of specific heats is $\gamma = 1.4$. It is common to take the initial position of the contact discontinuity as $x = 0.5$. The exact solution for this problem at $t = 0.25$ is shown in figure 8. As with the piston problem this can be used to investigate the effect of the viscosity formulation on the shock front, but in addition the viscosity should not affect the solution at the contact discontinuity or in the rarefaction wave.

Left	Right
$\rho_L = 1.0$	$\rho_R = 0.125$
$P_L = 1.0$	$P_R = 0.1$
$v_L = 0.0$	$v_R = 0.0$

Fig. 7 Initial conditions of the Sod shock tube problem.

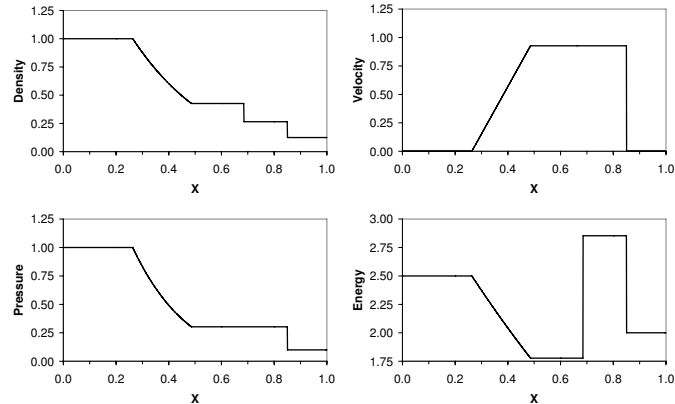


Fig. 8 Exact solution for Sod shock tube problem showing density, velocity, pressure and energy at time $t = 0.25$.

The Sod shock tube problem is an example of a 1D Riemann problem for the Euler equations which are commonly used for testing fluid dynamics codes [3].

3.2 Noh generic constant velocity shock

This problem, usually just called the Noh problem, has become a widely used test for hydrocodes since it was first described by Noh [7]. While it is a 1D problem there

are three variants, one in planar geometry, one in axi-symmetric geometry and the final in spherically symmetric geometry. In all three cases the problem consists of a region of cold ideal gas, $\gamma = 5/3$, with $\rho_0 = 1.0$ and $P_0 = 0.0$. The initial velocity $v_0 = -1.0$ everywhere. In all three cases the shock speed is $v_s = 1/3$, and all have constant post-shock conditions.

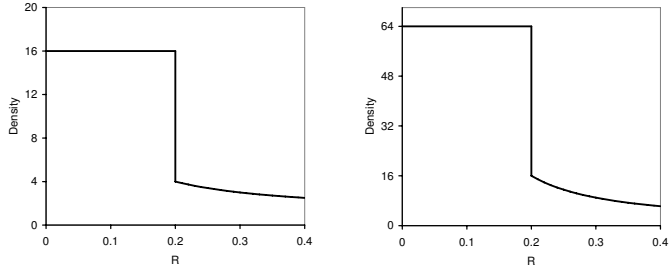


Fig. 9 The exact solution for density at $t = 0.6$ for Noh's axi-symmetric problem (left) and spherical problem (right).

The planar version is identical to the piston problem considered previously; the change is that is in a frame of reference where the piston is at rest. Exact results for the density at $t = 0.2$ is shown in figure 9 for the axi-symmetric and spherical cases. In both of these cases there is a region of uniform compression ahead of the shock, and especially with the spherical case the shockless Q heating error can be seen in this region.

Noh originally developed these problems to investigate the wall heating error. An example of the wall heating error can be seen in figure 10, showing results for the axi-symmetric problem calculated on a polar mesh. The effect of wall heating can be seen in the significant under-estimate of the density near the point of convergence in the numerical solution. The results shown use the edge viscosity formulation developed by Caramana [10].

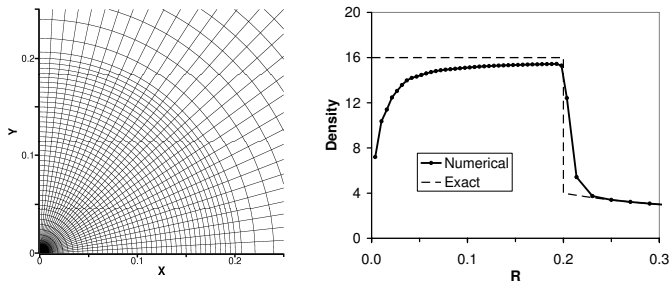


Fig. 10 Example axi-symmetric Noh problem results on a polar mesh (left) showing the density error due to wall heating (right). Solution time $t = 0.2$.

Another application of the Noh problem is to investigate the effect of mesh sensitivity when the shock propagates through a non-uniform mesh. The example shown in figure 10 used a polar mesh where the element edges are aligned with the flow and the mesh reflects the symmetry of the flow. For practical reasons it is rare to achieve this and using a rectangular mesh where all elements are initially square for the Noh problem can be used to investigate the consequences.

Figure 11 shows the results from a DYNA simulation of the axi-symmetric Noh problem. The elements are initially uniform cubes with symmetry boundary conditions used to enforce plane strain. The simulation used the standard viscosity (7) with the default values for the viscosity coefficients. The mesh sensitivity of the solution can be seen in both the mesh plot, especially along the 45 degree line, and in the scatter of the density results. The Noh problem does represent a tough problem for shock codes as it involves an infinitely strong shock and hence the level of mesh sensitivity is severe, but it must be understood that mesh sensitivity is present in all simulations that use the artificial viscosity method to capture the shock behaviour.

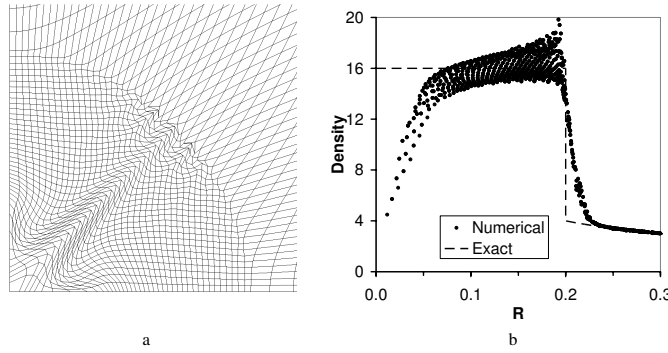


Fig. 11 Simulation results for the axi-symmetric Noh problem on a Cartesian mesh using the Von Neumann - Richtmyer viscosity at solution time $t = 0.2$. (a) Final mesh. (b) Plot of element density vs. radius for all elements.

3.3 Saltzman piston

The Saltzman piston problem [11] is a problem that has been widely used to test shock viscosities [10, 11, 12, 13, 14]. It tests the ability of a code to propagate a one dimensional shock through a two dimensional mesh. The initial conditions and analytical solution are identical to the piston problem considered earlier, however the initial mesh is different, figure 12. The mesh fills a rectangular domain that is 1.0 long by 0.1 high with 100 elements along the long edge and 10 elements along the short edge. The initial x coordinate of each node is defined in terms of their logical coordinates i and j as

$$x(i, j) = (i - 1)dx + (11 - j) \sin\left(\frac{\pi(i - 1)}{100}\right)dy, \quad (14)$$

where $dx = dy = 0.01$. The result of this is a distorted mesh, figure 12, although all elements have an aspect ratio close to one.



Fig. 12 Initial mesh for Saltzman piston problem

The standard viscosity is unable to preserve the one-dimensional solution, with the distortion of the mesh behind the shock clear in figure 13.

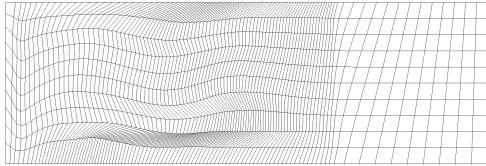


Fig. 13 Mesh at $t = 0.7$ for the Saltzman piston problem using the default DYNA viscosity.

The standard viscosity is unable to preserve the one-dimensional solution, with the distortion of the mesh behind the shock clear in figure. However the numerical solution remains a reasonable approximation to the analytical solution. Two variants of the Saltzman piston have been proposed, both alter the height of the rectangular domain leaving all other parameters unchanged. By altering the initial element aspect ratio both represent a tougher challenge for a viscosity than the standard test. In the first variant the height of the domain is increased by a factor of 100. This variant was originally proposed by Margolin [11] to investigate how very high aspect ratio elements affect the solution. The standard viscosity does not perform well on this problem [12] as the characteristic length calculated from the element volume

is much larger than the thickness of the element in the shock direction. In the second variant the height of the domain is reduced by a factor of 4. This variant was originally proposed by Campbell and Shashkov [14] to investigate how a moderate element aspect ratio affects the solution and to provide a greater degree of discrimination between viscosity forms. A further option with the Saltzman piston problem is to run the calculation past time $t = 0.75$. At this time the shock reaches the fixed end of the piston and is reflected. The reflected shock now propagates through mesh that has been distorted by the initial shock. Again this provides a greater challenge to the analysis code.

4 Alternative forms of artificial viscosity

The problems and errors resulting from the use of artificial viscosity have lead to the development of many different forms with varying properties. This section will briefly discuss two basic forms: the edge centred and the tensor viscosities, illustrating each with an example.

All forms of viscosity should satisfy the four conditions set out by Von Neumann and Richtmyer, see section 2 of this paper. More recently Caramana et al. [10] specified five additional properties that an artificial viscosity should possess, these are

1. Dissipativity: The artificial viscosity must only act to decrease kinetic energy.
2. Galilean invariance: The viscosity should vanish smoothly as the velocity field becomes constant.
3. Self-similar motion invariance: The viscosity should vanish for uniform contraction and rigid rotation.
4. Wave-front invariance: The viscosity should have no effect along a wave front of constant phase, on a grid aligned with the shock wave.
5. Viscous force continuity: The viscous force should go to zero continuously as compression vanishes and remain zero for expansion.

A viscosity that satisfies these conditions will not suffer from the shockless Q heating error and should show reduced mesh sensitivity over the standard form.

4.1 Edge centred viscosity

In an edge centred viscosity the viscosity force is calculated at an element edge rather than centred within an element. The strength of this approach is that the uncertainty over the choice of characteristic length in higher dimensions is removed, the length of the edge is now the natural choice. Each element edge connects two nodes and the forces resulting from the viscosity are directly applied to them. These forces should be applied in the direction of the relative velocity of the two nodes,

not along the line joining them. This change significantly improves the results and according to Margolin [11] is known as the Barton fix.

The viscosity developed by Caramana et al. [10] is an example of a modern edge viscosity that includes limiter terms. It is based on an alternative to equation (6) that was investigated by Wilkins [4] who attributed it to Kurapatenko [15].

$$q_{Kur} = \rho \left\{ c_2 \frac{(\gamma+1)}{4} |\Delta \mathbf{v}| + \sqrt{c_2^2 \left(\frac{\gamma+1}{4} \right)^2 (\Delta \mathbf{v})^2 + c_1^2 c_s^2} \right\} |\Delta \mathbf{v}| \quad (15)$$

where c_1 and c_2 are non-dimensional constants, γ is the ratio of specific heats and $\Delta \mathbf{v} = \frac{\partial \mathbf{v}}{\partial x} \Delta x$. This expression was derived from the pressure jump across a shock in an ideal gas. Wilkins shows that when simulating an ideal gas, using this viscosity removes the overshoot behind a shock.

In two dimensions the viscosity force for edge k of element e , that connects two nodes b and c , is

$$\mathbf{f}_k = \begin{cases} (1 - \psi_k) q_{Kur} (\widehat{\Delta \mathbf{v}_k} \cdot \mathbf{s}_c^e) \widehat{\Delta \mathbf{v}_k} & \text{if } (\Delta \mathbf{v}_k \cdot \mathbf{s}_c^e) < 0 \\ 0 & \text{if } (\Delta \mathbf{v}_k \cdot \mathbf{s}_c^e) \geq 0 . \end{cases} \quad (16)$$

\mathbf{f}_k then contributes to the total force at points b and c . Vector \mathbf{s}_c^e is a unit vector in the direction normal to the line connecting the mid-point of edge k to the centre of element e . The velocity difference for the edge is $\Delta \mathbf{v}_k = \mathbf{v}_b - \mathbf{v}_c$, and $\widehat{\Delta \mathbf{v}_k}$ is the unit vector in the direction of this velocity difference. For the edge the density and sound speed are

$$\rho_k = \frac{2\rho_b \rho_c}{\rho_b + \rho_c}, \quad c_{s,k} = \min(c_{s,b}, c_{s,c}). \quad (17)$$

The density and sound speed at a node is the volume weighted average of the surrounding elements. The function ψ_k is defined as

$$\psi_k = \max[0, \min(0.5(r_{l,k} + r_{r,k}), 2r_{l,k}, 2r_{r,k}, 1)], \quad (18)$$

$$r_{r,k} = \frac{\Delta \mathbf{v}_{k+1} \cdot \widehat{\Delta \mathbf{v}_k}}{\Delta \mathbf{x}_{k+1} \cdot \widehat{\Delta \mathbf{x}_k}} / \frac{|\Delta \mathbf{v}_k|}{|\Delta \mathbf{x}_k|}, \quad r_{l,k} = \frac{\Delta \mathbf{v}_{k-1} \cdot \widehat{\Delta \mathbf{v}_k}}{\Delta \mathbf{x}_{k-1} \cdot \widehat{\Delta \mathbf{x}_k}} / \frac{|\Delta \mathbf{v}_k|}{|\Delta \mathbf{x}_k|}. \quad (19)$$

Subscripts l and r refer to the left and right edges respectively. The left edge is found by considering all other edges that connect to node b and selecting the edge that forms the largest angle with edge k . The right edge is found in the same manner by considering edges that connect to node c .

The term ψ can be considered as a multi-dimensional form of a one dimensional TVD advection limiter. It acts to switch off the viscosity when the second derivative of the velocity field is zero and ensures that the viscosity satisfies the conditions of self-similar motion invariance and wave front invariance.

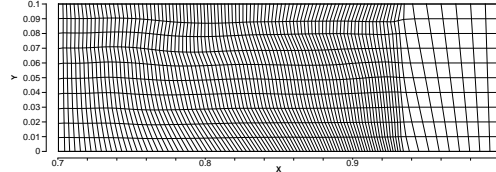


Fig. 14 Mesh at $t = 0.7$ for the Saltzman piston problem using the Caramana edge viscosity.

Results for the Saltzman piston problem using the Caramana edge viscosity are shown in figure 14, and shows a smoother solution than that obtained using the standard form, figure 13.

4.2 Tensor viscosity

In a tensor viscosity the scalar q term is replaced by a tensor \mathbf{Q} . The potential benefit of this change is that the effect of the viscosity can be directionally dependent, like an edge viscosity, while still being element centred. In addition there is no requirement that \mathbf{Q} be symmetric, and a nonsymmetric viscosity can remove mode conversion [11]. This means that for a shear flow in which all velocities are parallel, the viscous force will only act in the velocity direction. With a symmetric tensor viscosity the force would have a component perpendicular to the velocity direction.

The tensor viscosity developed by Campbell and Shashkov [14] is an example of a modern tensor viscosity that includes limiter terms. It assumes a form similar to physical viscosity, but based on \mathbf{L} rather than \mathbf{D} and so is not symmetric:

$$\mathbf{Q} = \mu \mathbf{L}^T. \quad (20)$$

μ is a scalar coefficient defined as

$$\mu = (1 - \psi) \rho \left\{ c_2 \frac{(\gamma+1)}{4} |\Delta \mathbf{v}| + \sqrt{c_2^2 \left(\frac{\gamma+1}{4} \right)^2 (\Delta \mathbf{v})^2 + c_1^2 c_s^2} \right\} l \quad (21)$$

where ψ is a limiter function similar to the function used in the Caramana edge viscosity although using the value of Δv in four directions rather than two.

Results for the Saltzman piston problem using this tensor viscosity are shown in figure 14, again showing a smoother solution than that obtained using the standard form. It should be noted that both the Caramana edge viscosity and this tensor viscosity are formulated within the framework of mimetic finite difference methods although there is no reason why they could not be extended to other numerical approaches.

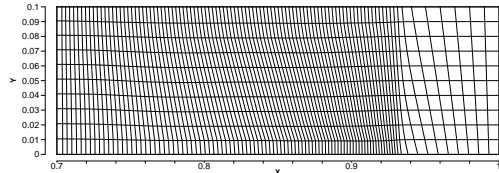


Fig. 15 Mesh at $t = 0.7$ for the Saltzman piston problem using the Campbell and Shashkov tensor viscosity.

5 Summary

This paper discusses the artificial viscosity method for the simulation of shock waves that is widely used today, especially for solid mechanics applications. The behaviour of the most widely available form of artificial viscosity is illustrated through a set of examples covering test problems that are commonly used to test different viscosity formulations. Finally other shock viscosity forms such as edge and tensor viscosities are briefly discussed.

References

1. Von Neumann J., Richtmyer R.D. (1950) A method for the calculation of hydrodynamic shocks. *J. Appl. Phys.* **21**, 232-237.
2. Godunov S. K. (1959) A difference scheme for numerical computation of discontinuous solutions of equations in fluid dynamics. *Mat. Sb.* **47**, 271-306.
3. Toro E.F. (1999) *Riemann Solvers and Numerical Methods for Fluid Dynamics*. Springer-Verlag Berlin Heidelberg
4. Wilkins M.L. (1980) Use of artificial viscosity in multidimensional fluid dynamic calculations. *J. Comput. Phys.* **36**, 281-303.
5. Landshoff R. (1955) *A numerical method for treating fluid flow in the presence of shocks*. LA-1930, Los Alamos National Laboratory.
6. Lin J.I. (2004) *DYNA3D: A nonlinear, explicit, three-dimensional finite element code for solid and structural mechanics*. UCRL-MA-107254, Lawrence Livermore National Laboratory.
7. Noh W.F. (1987) Errors for calculations of strong shocks using an artificial viscosity and an artificial heat flux. *J. Comput. Phys.* **72**, 78-120.
8. Rider W.J. (2000) Revisiting wall heating. *J. Comput. Phys.* **162**, 395-410.
9. Sod G.A. (1978) A survey of several finite difference methods for systems of nonlinear hyperbolic conservation laws. *J. Comput. Phys.* **27**, 1-31.
10. Caramana E.J., Shashkov M.J., Whalen P.P. (1998) Formulations of artificial viscosity for multi-dimensional shock wave computations. *J. Comput. Phys.* **144**, 70-97.
11. Margolin L.G. (1988) *A centered artificial viscosity for cells with large aspect ratios*. UCRL-53882, Lawrence Livermore National Laboratory.
12. Benson D.J. (1991) A new two-dimensional flux-limited shock viscosity for impact calculations. *Comput. Methods Appl. Mech. Engrg.* **93**, 39-95.
13. Benson D.J., Schoenfeld S. (1993) A total variation diminishing shock viscosity. *Comput. Mech.* **11**, 107-121.
14. Campbell J.C., Shashkov M.J. (2001) A tensor viscosity using a mimetic finite difference algorithm. *J. Comput. Phys.* **172**, 739-765.

15. Kurapatenko V.F. (1967) *In: Difference methods for solutions of problems of mathematical physics, I* (Editor: N.N. Janenko). Amer. Math. Soc., Providence, R.I., p. 116.